MOLECULAR ECOLOGY

Molecular Ecology (2009) **18**, 4775–4789 doi: 10.1111/j.1365-294X.2009.04382.x

Source–sink dynamics structure a common montane mammal

KIM O'KEEFE,* UMA RAMAKRISHNAN,† MARCEL VAN TUINEN‡ and ELIZABETH A. HADLY*

**Department of Biology, Stanford University, Stanford, CA 94305-5020, USA, †National Center for Biological Sciences, TIFR, GKVK Campus, Bellary Road, Bangalore 560065, India, ‡Department of Biology and Marine Biology, University of North Carolina at Wilmington, Wilmington, NC 28403, USA*

Abstract

Assessing the relative role of evolutionary processes on genetic diversity is critical for understanding species response to climatic change. However, many processes, independent of climate, can lead to the same genetic pattern. Because effective population size and gene flow are affected directly by abundance and dispersal, population ecology has the potential to profoundly influence patterns of genetic variation over microevolutionary timescales. Here, we use aDNA data and simulations to explore the influence of population ecology and Holocene climate change on genetic diversity of the Uinta ground squirrel (*Spermophilus armatus*). We examined phylochronology from three modern and two ancient populations spanning the climate transitions of the last 3000 years. Population genetic analyses based on summary statistics suggest that changes in genetic diversity and structure coincided with the Medieval Warm Period (MWP), *c.* 1000 years ago. Serial coalescent simulations allowed us to move beyond correlation with climate to statistically compare the likelihoods of alternative population histories given the observed data. The data best fit source–sink models that include large, mid-elevation populations that exchange many migrants and small populations at the elevational extremes. While the MWP is likely to have reduced genetic diversity, our model-testing approach revealed that MWP-driven changes in genetic structure were not better supported for the range of models explored. Our results point to the importance of species ecology in understanding responses to climate, and showcase the use of ancient genetic data and simulation-based inference for unraveling the relative roles of microevolutionary processes.

Keywords: aDNA, climate change, metapopulation, population structure, serial coalescent, Serial SimCoal

Received 22 November 2008; revision received 1 August 2009; accepted 29 August 2009

Introduction

One objective of evolutionary studies is to better understand how species respond to changes in their environment. Phylogeographic studies of modern genetic variation often reveal correlations between patterns of genetic diversity and structure and known climatic events such as glaciation (e.g. Avise 2000; Demboski & Sullivan 2003; Eddingsaas *et al.* 2004; Hewitt 2004). However, at the population level, several microevolutionary and ecological processes independent of climatic change can give rise to the same modern genetic patterns. Assessing the relative role of different processes on standing genetic diversity is critical for understanding how species will respond to climatic changes. For example, low genetic structure between modern populations could result from recent geographic separation, high gene flow and/or selection. It is difficult to distinguish between these possibilities with modern genetic data alone. Not all past events leave discernable marks on modern populations, because they proceeded too

Correspondence: Kim O'Keefe, Fax: 650-725-8221;
E-mail: kokeefe@stanford.edu

rapidly or have been masked by more recent events (Ramakrishnan & Hadly 2009). In addition, although population genetic analyses have been valuable for identifying recent population declines related to human activities (e.g. Goosens *et al.* 2006), they lack power to discriminate older population processes or multi-event population histories.

Analysis of ancient DNA (aDNA) has profoundly changed our ability to explore genetic response to climatic change by allowing us to track population-level changes directly through time (Ramakrishnan & Hadly 2009). Several aDNA studies have revealed cryptic events such as population bottlenecks (Chan *et al.* 2006), loss of genetic diversity (Leonard *et al.* 2007) and population extinction (Dalen *et al.* 2007). In addition, aDNA has improved the ability to ascertain the timing of genetic changes and how well those shifts match the timing of known climatic events. A recent review of aDNA studies highlighted the utility of temporal genetic data for revealing population processes and outlined a novel simulation-based approach for comparing the likelihood of alternate demographic histories (Ramakrishnan & Hadly 2009). Although several modern (Hadly *et al.* 2003; Goosens *et al.* 2006) and aDNA studies summarized in Ramakrishnan & Hadly (2009) revealed past changes in population size, change in gene flow through time was found less often (see Leonard *et al.* 2000; Barnes *et al.* 2002; Valdiosera *et al.* 2007, 2008). The genetic consequences of even more complex (but perhaps more realistic) demographic scenarios, including changes in both population size and gene flow, remain challenging to explore.

The Greater Yellowstone Ecosystem (GYE) and its core, Yellowstone National Park (YNP), protect one of the most species-rich intact temperate ecosystems in North America (Hadly 1996). However, as recently as 12 000 years BP, YNP was covered by an icecap (Pierce 1979; Fig. 1A). The flora and fauna of the GYE are thus only recently assembled, having colonized the area following the retreat of the ice (Bruzgul & Hadly 2006). One colonizer, the Uinta ground squirrel (*Spermophilus armatus:* genus *Urocitellus sensu* Helgen *et al.* 2009), is now one of the most abundant and ubiquitous mammals in the GYE (Streubel 1989). Uinta ground squirrels form colonies in mountain meadows from 1219 m to timberline (Howell 1938). A paleontological study of the

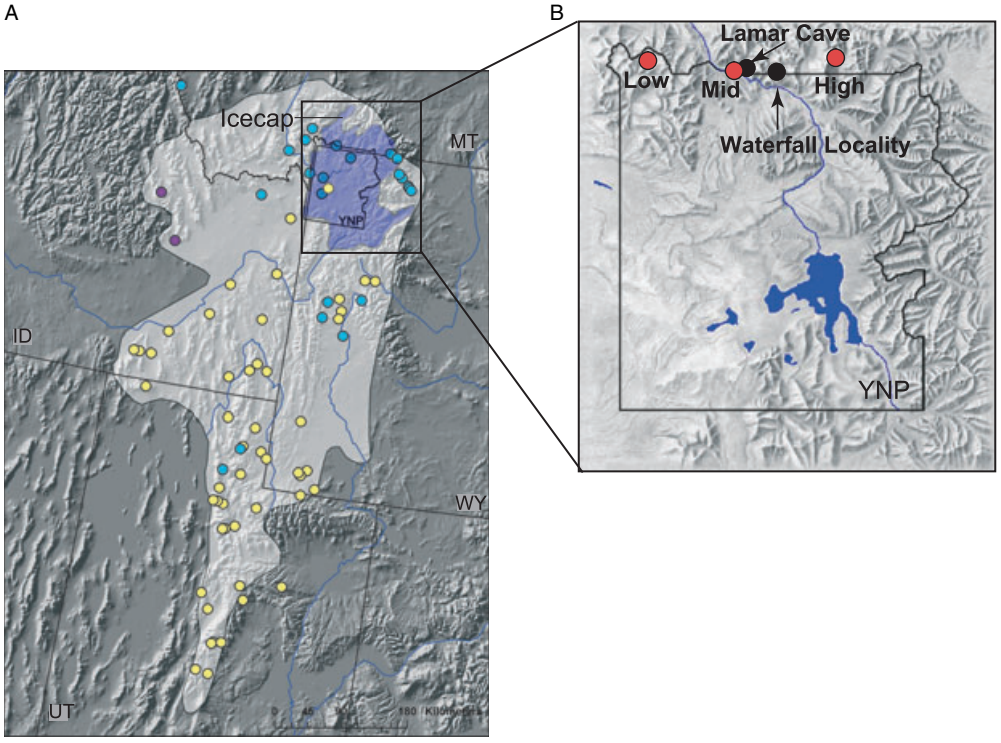

Fig. 1 (A) Map of *Spermophilus armatus* distribution (grey-shaded relief) and the Icecap (blue-shaded relief) over Yellowstone National Park (YNP) during the late Pleistocene and until *c.* 12 000 years BP (adapted from Pierce 1979). Colours represent the three genetic lineages found within the species range (adapted from van Tuinen *et al.* 2008): Northwestern lineage = NWL (purple), Northeastern lineage = NEL (blue), and Southern lineage = SL (yellow). (B) Map of sampling localities in Yellowstone National Park at 45°N latitude. Modern sites are shown in red (Low, Mid and High). Fossil sites are shown in black (Lamar Cave and Waterfall locality).

mammals of YNP showed that *S. armatus* has been present for at least 3000 years (the maximum age of the Holocene vertebrate record in YNP) and that *S. armatus* increased in abundance in response to late-Holocene warming during the Medieval Warm Period (MWP) (Hadly 1996). A phylogeographic study of *S. armatus* (van Tuinen *et al.* 2008) revealed admixture near the GYE suggesting dispersal between regions. Because effective population size and gene flow are affected directly by abundance and dispersal, population ecology has the potential to profoundly influence patterns of genetic variation over microevolutionary timescales (Avise 2000, p. 37) and may influence genetic diversity in this species.

We tracked the genetic diversity and population structure of the Uinta ground squirrel from both modern and ancient populations spanning the climate transitions of the late Holocene in the GYE. Using a two-step analytical process, we investigated whether population structure had changed through time and if so, whether this change was best explained by the climatic transition of the MWP. First, we analysed our modern and aDNA data using traditional phylogenetic and population genetic approaches focused on measures of genetic diversity and standard population parameters. Next, we used serial coalescent simulations to explore more complex models of population history that might have led to the observed genetic patterns. Analysing our ancient genetic data in this model-testing framework (Ramakrishnan & Hadly 2009) also allowed us to investigate the effects of demographic changes associated with or independent of climatic change. The deglaciation of the Yellowstone plateau 12 000 years ago (allowing a known 'starting-point' for our models) combined with a rich fossil data set and a modern protected ecosystem provided us with the opportunity to explore the genetic consequences of demography and climatic change on this species.

Materials and methods

Sampling

We sampled three modern and two ancient populations along a west-to-east elevational gradient in and around northern YNP (Fig. 1B). Based on extensive ground surveys and inspection of topographic maps, these populations encompass the elevational extremes for *Spermophilus armatus* at this latitude (45°N). The population at the lowest elevation ('Low site') occurs at 1707 m in a shallow drainage near Gardiner, Montana (GPS: 12T 055007 UTM 4974241). The mid-elevation population in Lamar Valley ('Mid site') occurs at the centre of the elevational range of the species at 1890 m (GPS: 12T 0541010 UTM 4974306). The Mid site is just outside Lamar Cave (12T 0550828.43 UTM 4974024.06), permitting a comparison with available ancient samples for the population (Hadly 1996). Lamar Cave contains a well-stratified, radiocarbon-dated accumulation of deposits comprised of local species in the vicinity, including *S. armatus* (n = 1849; Hadly 1996, 1999). The cave deposits continuously span the last 3000 years and thus record *S. armatus* as it experienced the climate transitions of the MWP (1150–650 years BP; Soon & Baliunas 2003). A second opportunity to track the ancient population genetic response to the MWP is provided by ground squirrel specimens excavated from Waterfall Locality (Porder *et al.* 2003; Hadly & Steele, in prep), which dates from just older than 3000 years BP to the present. Waterfall Locality is at 1875 m (GPS: 12T 0573828.43 UTM 4978852.69) in a drainage of Soda Butte valley. We found no evidence of an extant population after an extensive survey for calls, burrows and animals in the vicinity of Waterfall Locality during the summer of 2002. No active colonies were detected in the vicinity during subsequent summers 2003 and 2004. Thus, we surmised that this population is currently extinct. Our third modern study population at this latitude is located at the highest elevation ('High site'), occurring at 2683 m in the Beartooth Mountains (GPS: 12T 0607199 UTM 4976050). A straight-line distance of 28 km separates the Low site from the Mid site (and Lamar Cave), and 57 and 42 km separate the High site from the Mid site and Waterfall Locality respectively.

Sampling of populations

We live-trapped ground squirrels from each of the three modern populations using Sherman™ folding live traps (XLF 15) baited with oats and peanut butter. Each captured animal was given a unique Monel No. 1 ear tag (National Band and Tag Company) to avoid resampling the same individual. A small ear snip was taken from 192 individuals, stored in 90% EtOH and taken to the lab for genetic analysis. We sampled *S. armatus* specimens from several radiocarbon-dated stratigraphic levels in Lamar Cave and Waterfall locality following Hadly (1996). We limited our aDNA sampling to the first or second molar from the left jaw (depending on sample size per level) to avoid sampling the same individual multiple times.

Laboratory methods

We extracted modern DNA using the QIAGEN DNeasy® extraction kit following the manufacturer's protocol for purification of total DNA from animal tissues. We used hot-start polymerase chain reaction

(PCR) with Taq Gold™ to amplify two regions of the mitochondrial genome. First, 634 base pairs (bp) of the control region (CR) were obtained using the forward primer Pro5sciurus (5′-CACCTTCAACTCCCAAAGC-3′; Brahic and Spicer, personal communication), and reverse primers Sarm5 (5′- CCACTAAAGGCATGACAGTGC-3′) and SarmD1 (5′-AGTTATGTTGGGTCACGGGCTAA-3′), yielding 548 bp of homologous CR sequences. Second, 633 bp of the cytochrome *b* (cyt*b*) gene were obtained using the forward primer Sarm9 (5′-TCTTTTATCCGCTATTCCGTAC-3′) and the reverse primer Sarm4 (5′-TTTTCGATTAGGCTGACGGTTGG-3′) that yielded a 511-bp fragment of homologous cyt*b* sequences. PCR cycles for the CR fragment were run as follows: denaturation at 95 °C for 10 min, followed by 30 cycles of 95 °C for 45 s, 55 °C for 45 s and 72 °C for 2 min with a final extension at 72 °C for 5 min. PCR cycles for cyt*b* were as follows: 10 min denaturation at 95 °C, followed by 36 cycles of 94 °C for 30 s, 50 °C for 45 s and 72 °C for 1 min with a final extension at 72 °C for 10 min.

aDNA extraction, amplification and contamination control followed the published protocol by Hadly *et al.* (2004). We used the previously developed primer pairs Sarm1-2, Sarm3-4, Sarm 10-11, SarmD10-11 and SarmD12-13 (van Tuinen *et al.* 2008), which yielded 263 bp of homologous CR and 359 bp of cyt*b* sequences. Sequencing was outsourced (Cogenics). All sequences were aligned and analysed in the program Sequencher 4.7 (GeneCodes). Authentication of all mitochondrial sequences followed van Tuinen *et al.* (2008) and included the use of multiple contamination controls, spatial separation of modern and ancient samples, reagents and personnel, sequencing forward and reverse directions, and repeating extraction and amplification of unique ancient haplotypes. Three ancient samples were independently verified in a second genetic lab located in a different building with separate reagents and facilities (U. Ramakrishnan Lab, NCBS, India). Variable sites were visually verified and cyt*b* sequences were translated to their amino acid sequences to confirm proper coding status. Control region PCR products from two representatives from each of the two most divergent modern lineages were cloned (TOPO TA) to check for the presence of numts and confirm authenticity. No anomalous sequences were detected to suggest the presence of numts sequences in our data.

Phylogenetic and population genetic analyses

Phylogenetics and genetic diversity. Phylogenetic analyses to determine lineage association of ancient and modern haplotypes followed van Tuinen *et al.* (2008) with modifications to handle the increased computational time for analysis. Analyses were performed in PAUP 4.0beta (Swofford 2003) and MEGA 4.1. The neighbour-joining (NJ) tree was constructed using maximum composite likelihood distances (Tamura *et al.* 2004) calculated using models and parameters (CR: Tamura-Nei, $\alpha = 0.19$; cyt*b*: HKY, *T*-ratio = 22.6) established from the Akaike Information Criterion in ModelTest 3.3 (Posada & Crandall 1998). Observed indels were recoded as additional transitions to account for this variation in subsequent analyses (for similar approaches see Vargas *et al.* 1999; Simmons & Ochoterena 2000). To ascertain nodal support and permit additional searches across tree space, bootstrap values were noted between phylogenies resulting from the NJ analysis, maximum parsimony (MP) and maximum likelihood (ML) phylogenies. MP analyses were run in PAUP 4.0 beta using both the NJ tree and random starting trees, and 500 bootstrap iterations. ML analyses were run in GARLI (Version 0.96; http://www.nescent.org) using initial settings and nucleotide substitution model rate parameters inferred from ModelTest (see above). In order to reduce the probability that an individual search was trapped in a local optimum, we performed 500 bootstrap replicates with two search replicates per bootstrap (Zwickl 2006). A majority rule consensus tree was generated for each dataset using PAUP 4.0beta (Swofford 2003).

Our primary focus was to investigate demographic changes in this species through time. Because the CR sequences highlighted considerably more substitutional variation than cyt*b* sequences (up to 7 times more: van Tuinen *et al.* 2008), we limited our demographic analyses and simulations to the CR data. Genetic sample sizes for each population were as follows: Low site (modern only, $n = 31$); Mid site (modern, $n = 45$; ancient, $n = 55$); Waterfall Locality (ancient only, $n = 29$); High site (modern only, $n = 29$).

Traditional phylogenetic approaches assume a bifurcating pattern of genetic divergence that may not accurately reflect intraspecific patterns of genetic diversity in which ancestral and more derived haplotypes may be present in the same population (Posada & Crandall 2001). Therefore, we also performed a statistical parsimony (SP) analysis in TCS (Clement *et al.* 2000) to generate an unrooted haplotype network using a 95% cutoff. Woolley *et al.* (2008) found that SP from the TCS software had lower error than several other network methods evaluated.

For comparison with results obtained through simulations, we calculated standard estimates of intrapopulation genetic diversity using a simple pairwise distance model. To estimate effective population sizes we estimated mutation rate for the CR data. Direct

Table 1 Mitochondrial DNA (mtDNA) haplotypes for the cytochrome *b* (cyt*b*) and control region (CR) for each of three modern populations and two ancient populations of *Spermophilus armatus* from the Yellowstone region (described in text)

Population	cyt*b* (n = 170 samples)	CR (n = 189 samples)
Modern		
Low	A1, A2(25)	A9(3), A12, A13(7), A15(19), A22
Mid	A1(4), A2(12), A3(5), B1(19)	A1(3), A4(3), A8(5), A21(14), B22(2), B23(2), B25(14), B27(2)
High	A1(13), A3(9), A4(4)	A1(25), A3(4)
Ancient		
$LC_{MWPandpost}$	A1 (6), A3 (5), A6 (1), B1 (22), B3, B4, B5, B7	A1(6), A8, A9(6), B20(3), B22(13), B25(12), B26
$LC_{pre\text{-}MWP}$	A2(2), B1(2), B2, C1(5), C2, C4	A16, A19, B19, B20, B25, B28, C4(6), C6
$WF_{MWPandpost}$	A1(3), A4, C1(2)	A1(3), A3, C3(2)
$WF_{pre\text{-}MWP}$	A1(7), A6, B1(4), C1(8), C2	A1, A8(6), A9(2), B20(4), B29, C2, C3(2), C4(6)
Total (bp)	359	263

Numbers in parentheses are frequencies >1. The letters correspond with the previously identified lineages: A = Northeastern lineage (NEL), B = Southern lineage (SL), C = Northwestern lineage (NWL).

calibration of the mutation rate in the CR fragment for *S. armatus* is ineffective because of an incomplete fossil record and extensive variation in CR evolutionary rates among close lineages (Ho *et al.* 2005). Therefore, following van Tuinen *et al.* (2008), we estimated the average observed substitution rate relative to the cyt*b* substitution rate and converted this to an absolute rate based on a 1.52%/Myr rate for *Spermophilus* cyt*b* (Eddingsaas *et al.* 2004). Effective population size (N_e) was estimated using the following equation: $N_e = \theta_{(\text{homozygosity} \pm \text{SD})}/2(\mu)$. Mutation rate was not rescaled because squirrel generation time is 1 year (Millar & Zaummuto 1983). Heuristic searches were performed using ML with and without a molecular clock constraint. A likelihood ratio test under a chi-squared probability distribution was used to assess significant departure from a clock-like model of evolution (Huelsenbeck & Crandall 1997). To test for changes in effective population sizes, we used Tajima's *D* (Tajima 1989a,b) and Fu's neutrality test (Fu 1997) in Arlequin 3.1 (Excoffier *et al.* 2005), which is a particularly powerful test for detecting sudden and recent expansions in populations with an excess of rare alleles.

Genetic differentiation and population structure Population structure was determined by analysis of molecular variance (AMOVA) in Arlequin 3.1 (Excoffier *et al.* 2005). AMOVA uses the frequency of haplotypes and the number of nucleotide differences between them to test the significance of the partitioning of variance between predefined hierarchical groups (among groups Φ_{CT}, among populations within groups Φ_{SC} and with populations Φ_{ST}; Excoffier *et al.* 1992). Once we determined the population structure that partitioned the most variance among groups, we calculated pairwise F_{ST} values between all populations. We also tested for differentiation between groups based on haplotype frequencies using the exact test of differentiation (Raymond & Rousset 1995).

Modelling

Simulations. Serial coalescent simulations can model genetic samples from different points in time and space (Drummond *et al.* 2002; Ramakrishnan *et al.* 2005). Using the serial coalescent as implemented in Serial SimCoal (Anderson *et al.* 2005; Ramakrishnan & Hadly 2009), we investigated whether the observed data fit a range of simple or more complicated models of population history. Genetic samples were partitioned into three time intervals: (i) pre-MWP (aDNA from Lamar Cave and Waterfall Locality), (ii) MWP to present (aDNA from Lamar Cave and Waterfall Locality), and (iii) present (modern DNA from the Low, Mid and High sites). We initially investigated three simple models of population history ranging along the spectrum from panmixia to complete isolation. All simple models (except panmixia) assume four populations of equal size (Table 2, model A) that correspond with the populations we sampled [Low, Mid (includes Lamar Cave), Waterfall Locality and High]. Models with complete isolation assume no gene flow following colonization of previously glaciated portions of the GYE. The intermediate models such as those with migration following isolation also assume equal, bidirectional migration rates between neighbouring populations. All simulations were carried out at a range of parameter values (N_e between 2000 and 500 000 for each population and migration rate between 1 and 5 migrants per generation for the isolation–migration models). For simplicity, we assumed that the GYE was colonized 12 000 years ago following melting of the Yellowstone icecap and that the populations split (in cases of complete isolation and

isolation migration models) 10 000 years ago. In all cases, simulations were repeated 5000 times. These simple demographic models are represented in Table 2, model A.

We investigated two more complex population genetic models, including (i) models with asymmetry in population size and gene flow between populations (Table 2, model B) and (ii) models where gene flow, and thus population structure, changed during the history of these populations (Table 2, model C). The first category of models investigated possible source–sink dynamics, which is suggested by ecological studies on

Table 2 Likelihood estimates for various demographic models and their Akaike information criterion (AIC) values

	Model	Likelihood	Parameters	AIC	Δ AIC
A	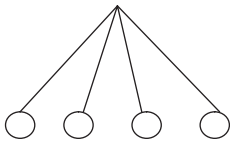	6.23×10^{-30}	2 N_e, population divergence	62.41	35.07
	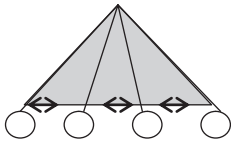	1.83×10^{-31}	3 N_e, population divergence, migration rate	67.47	40.13
B	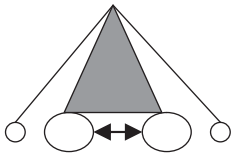	2.11×10^{-10}	4 N_e central populations, N_e peripheral populations, population divergence, m central populations	**27.34***	
	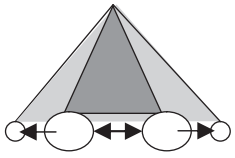	4.84×10^{-15}	5 N_e central populations, N_e peripheral populations, population divergence, m central populations, m peripheral populations	38.63	11.28
C	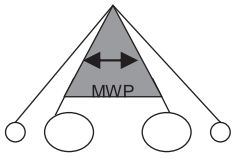	4.14×10^{-15}	5 N_e central populations, N_e peripheral populations, population divergence, m central populations, cessation of gene flow	38.76	11.42
	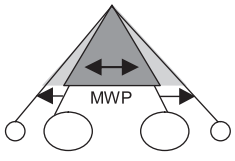	1.51×10^{-15}	6 N_e central populations, N_e peripheral populations, population divergence, m central populations, m peripheral populations cessation of gene flow	41.64	14.29

The most likely model (AIC=27.34) is one with four parameters, including asymmetrical core population sizes, with high gene flow between central populations only. Circles denote populations and their relative size; arrows indicate direction and timing of gene flow. A:simple models assuming populations of equal size and either no gene flow or equal gene flow between populations; B:more complex models with asymmetry in population size and gene flow between populations (to investigate potential source—sink dynamics); C:models where gene flow, and thus population structure, changed during the history of these populations [to investigate changes in population structure and diversity driven by the Medieval Warm Period (MWP)].
*the most likely model.

this species (K. O'Keefe & E. A. Hadly, unpublished; Table 2, model B), whereas the second set of models investigated potential changes in population structure and diversity driven by the impacts of climate experienced during the MWP (Table 2, model C). These more complex models assumed that mid-elevation sites (modern Mid site in Lamar Valley, and prehistoric Lamar Cave and Waterfall Locality sites) had 2, 5 or 10 times higher effective size than the Low and High sites. Additionally, we assumed that the mid-elevation sites exchanged migrants at a high rate (bidirectional gene flow of 10 migrants per generation). We also investigated models where gene flow to the high and low elevation sites was unidirectional (allowing these sites to function as 'sinks') from the mid-elevation sites. We modelled the possible impacts of the MWP by changing population structure following this climatic event. In the investigation of the role of climate, we modelled a cessation of gene flow from 1000 years BP to the present.

Statistical analyses

We evaluated the statistical fit of these five different models to the observed genetic data using empirical likelihoods as calculated in Belle *et al.* (2006) and Ramakrishnan & Hadly (2009). For each set of calculations, we used 19 statistics, which included five F_{ST} values and 14 intra-population statistics. Inter-population statistics included pairwise F_{ST} between the three modern populations and between Lamar and Waterfall during the two ancient sampling periods. Intra-population statistics included average pairwise difference and number of segregating sites for two ancient populations (during both time periods) and the three modern populations. The highest likelihood values were used to calculate the AIC value (Burnham & Anderson 2002), and models were compared using differences in AIC values.

Results

Phylogenetic and population genetic analyses

Genetic variation. Sequencing of the CR and cyt*b* fragments of modern and ancient individuals combined resulted in 25 and 14 haplotypes respectively (GenBank accession EU035712–EU035751; Table S1; Table 1). We sequenced the CR for 189 individuals (modern $n = 105$; ancient $n = 84$) and cyt*b* sequences from a subset of those individuals (modern $n = 92$; ancient $n = 78$ of which 167 individuals overlapped with the CR dataset). The number of segregating sites varied between the two loci (CR > cyt*b*). The CR had 32 segregating sites from the modern and 35 segregating sites in the ancient samples. cyt*b* was less variable and had eight segregating sites from the modern individuals and 12 segregating sites from the ancient individuals. Phylogenetic analyses revealed low variation in cyt*b* (average pairwise divergence =3%) and tentative geographic clustering of *S. armatus* into three lineages. These lineages correspond to the three lineages detected previously in a phylogeographic study (Figs. 1B; Fig. 3A in van Tuinen *et al.* 2008) and here we followed the same nomenclature: Northwestern lineage (NWL), Northeastern lineage (NEL) and Southern lineage (SL). The faster-evolving CR harboured more phylogenetic information (average pairwise divergence = 18%), and yielded the same geographic clustering among *Spermophilus armatus* as did cyt*b* (Fig. 2B). Despite low support, the topological consistency between the linked genes bolsters our confidence (in addition to the other measures we have taken) that we have authentic sequence data.

When all individuals were analysed simultaneously, the unrooted haplotype cladogram again resolved three distinct lineages (NEL, NWL and SL; see Table 1 for haplotypes frequencies). To better visualize the data, we generated haplotype networks for each of the populations separately (Fig. 3). The network analyses do not reproduce the relationships among the three lineages that phylogenetic analyses revealed. Woolley *et al.* (2008) showed that tree approaches (e.g. MP) are better for inferring relationships between lineages. Thus, for the relationships among the three lineages, we refer to the phylogenetic analyses performed in van Tuinen *et al.* (2008), which encompassed the entire species range and benefited from the inclusion of an outgroup (*Spermophilus beldingi*). The networks are ideal for visualizing how genetic diversity is partitioned in both space and time. Figure 3 shows that all modern populations (Low, Mid and High) contained individuals from the NEL (blue). The modern Mid site also had individuals from the SL (yellow), as did both of the paleontological sites (Lamar Cave and Waterfall Locality). Both the ancient localities also had individuals from the NWL (purple), which appears to have become extinct just prior to the MWP in Lamar Valley and during the MWP (*c.* 1000 years BP) at Waterfall Locality. Despite extensive sampling, we found no evidence for the presence of individuals from the NWL anywhere in the modern range of the species, except in the northwestern-most part of its historic range from the 1930s, on the margins of the species range (van Tuinen *et al.* 2008). The species is not known from this location in Idaho since the 1930s, suggesting that this clade is extinct today (van Tuinen *et al.* 2008).

After correction for intra-site polymorphism, the average divergence between populations for CR was estimated at 1.86×10^{-4} substitutions per site. Intra-site

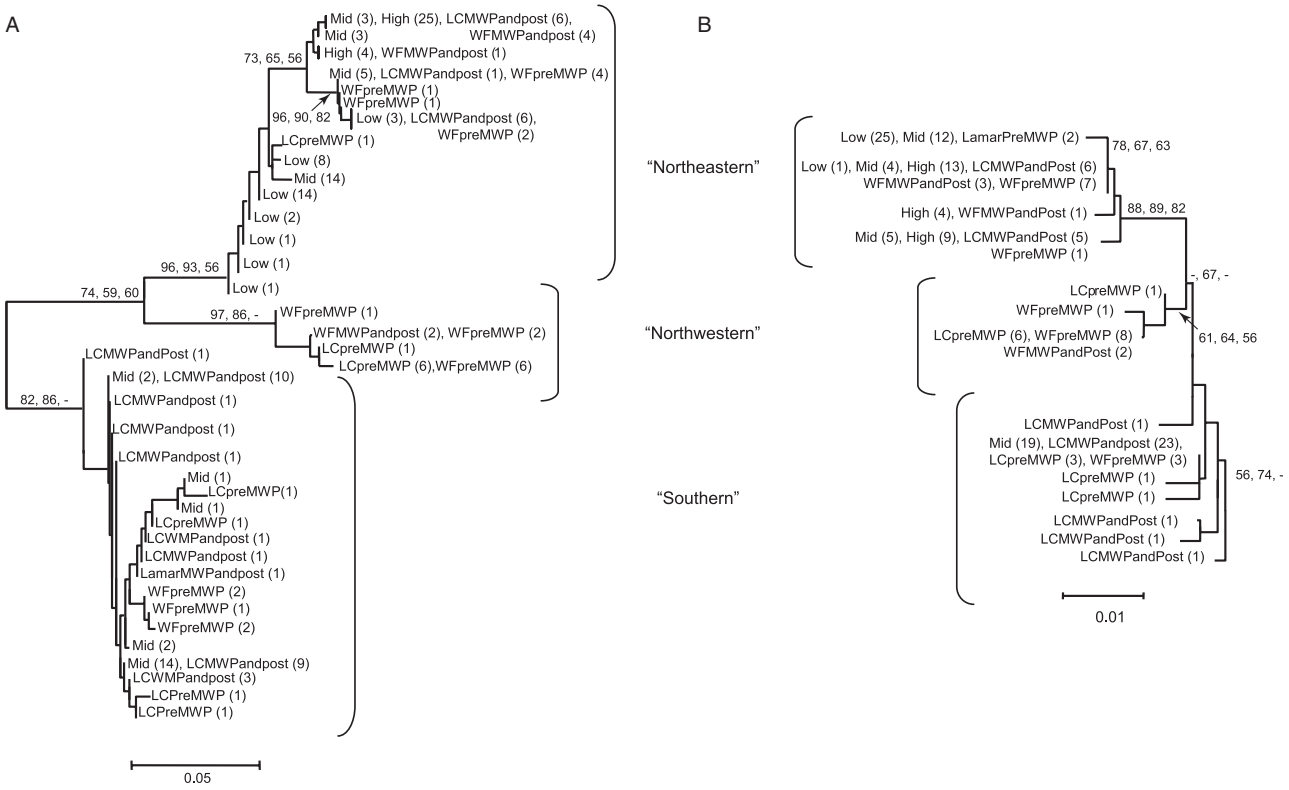

Fig. 2 Topology of DNA sequences from modern and ancient individuals of *Spermophilus armatus* sampled in or nearby Yellowstone National Park. (A) Phylogenetic tree based on CR sequences (262–263 bp). Depicted is the neighbour-joining tree using a TN+G ($\alpha = 0.19$) model as specified by ModelTest (van Tuinen *et al*. 2008). Numbers shown above the nodes are: bootstrap values using maximum parsimony (500 iterations), bootstrap values using neighbour-joining (500 iterations) and bootstrap values using maximum likelihood (2 replicates, 500 iterations). Modern DNA sequences derive from individuals live-trapped at Low, Mid and High elevation sites; ancient DNA sequences are from Lamar Cave (LC) and Waterfall Cave (WF), either predating the Medieval Warm Period (preMWP), or since the MWP (MWPandpost). (B) Phylogenetic tree based on cyt*b* sequences (359 bp). Depicted is the neighbour-joining tree using the HKY model and a transition:transversion ratio = 22:1. Note the lineage consistency across linked markers in spite of large differences in mutation rate.

genetic diversity indices also differed between the populations (Table S2). Both Low and High sites were characterized by relatively low diversity values (Table S2) and low haplotypic diversity (percent unique haplotypes = 2% and 7% respectively) with haplotypes represented only from the NEL. In contrast, the middle elevation sites, present and past (Mid site in Lamar Valley, Lamar Cave and Waterfall Locality), maintained relatively high diversity values (Table S2) and had higher haplotypic diversity (17%, 39% and 42% respectively). The latter localities also contained individuals from the NEL and the SL. In addition, the pre-MWP ancient populations included the now extinct NWL. Assuming an average mutation rate (μ) for the CR of 3.68×10^{-5} per year (see van Tuinen *et al*. 2008), effective population size estimates based on θ (homozygosity) for the modern and ancient populations at different time points varied considerably (Table S2). Although calculation of effective size can be inaccurate due to uncertainty in mutation rate, we focused on the relative differences of N_e between populations. Populations at the elevational extremes (Low site and High site) had lower N_e (3 and 13 times lower respectively) than the populations at the Mid site. Rapid historic changes in population size were not detected from either Fu's F_s values or Tajima's D values (Table S2).

Genetic differentiation and population structure. Grouping individuals into three geographically defined modern populations and two geographically defined ancient populations, each separated into two time periods (one pre-MWP and one post-MWP) produced the highest Φ_{sc} and explained 36% of the genetic variation among groups ($F_{ST} = 0.363$, $P < 1.0 \times 10^{-4}$) (see Table S3 for other tests of groupings). Significant F_{ST} values were found between all the modern population pairs and between the two ancient populations following the climate transition of the MWP ($LC_{MWPandpost}$,

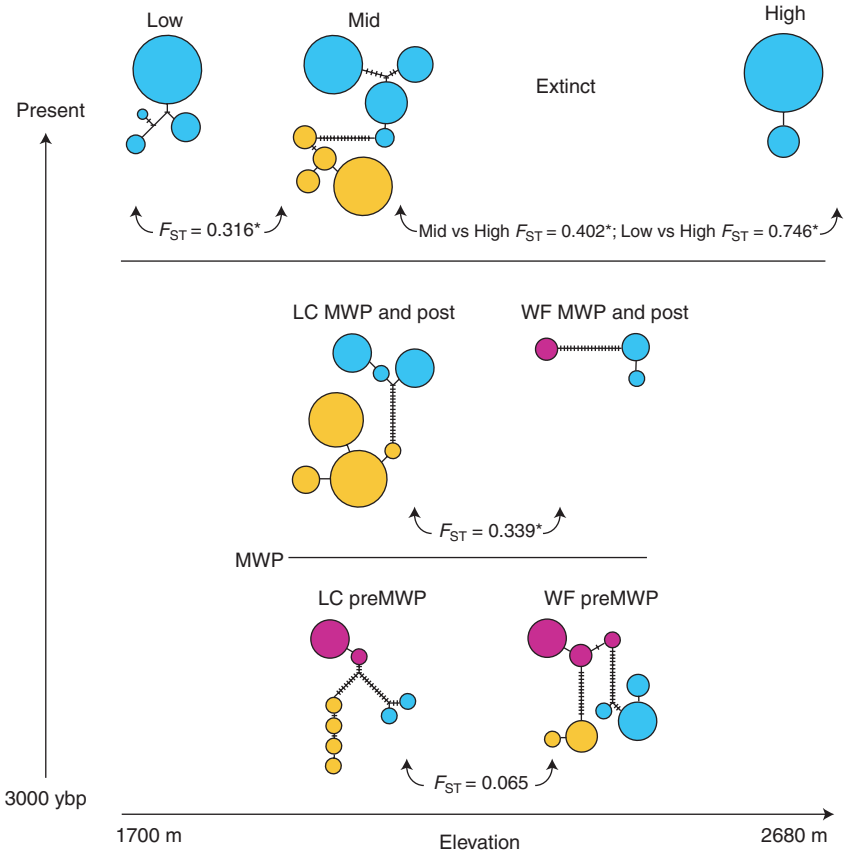

Fig. 3 Unrooted haplotype networks of absolute distances between mitochondrial DNA haplotypes of the CR. Each circle represents a unique haplotype, its size proportional to haplotype frequency. Colours represent the three genetic lineages from different geographic areas within the species range from analysis of all sequences in TCS: NWL (purple), NEL (blue) and SL (orange). Lines connecting each haplotype represent a single nucleotide substitution, and the hatch marks along those branches represent additional substitutions. Pairwise F_{ST} values between populations compared in the simulations are included below and between the networks. Asterisks denote $P < 0.05$.

$WF_{MWPandpost}$) (Fig. 3). Before the MWP, we detected no significant structure between the ancient populations (LC_{preMWP}, WF_{preMWP}). The population structure of Waterfall Locality did not change after the MWP ($WF_{preMWP} = WF_{MWPandpost}$), although no population is found in the vicinity of Waterfall Locality today. Finally, the modern Mid site was not significantly different from the nearby ancient WF locality after the MWP (Fig. 3). Exact tests of population differentiation (Raymond & Rousset 1995) were significant for all population pairs. These results suggest that population structure at the Mid site changed around the time of the MWP. We further investigated the likelihood that the climatic transition of the MWP best explains the coincident change in population structure using simulations. Our simulations were also intended to explore how differential population size and gene flow may influence results based on parameter estimation as interpretations from F_{ST} values assume constant size and gene flow and simulations are free of this constraint.

Modelling

Simple models. Simulation results, presented as shaded cells in Fig. 4A, allowed visualization of the parameter space for low (2000), intermediate (50 000) and high (100 000) values of effective size for all three simple models (panmixia, isolation migration and complete isolation). For these simulations, we assumed equal population sizes and equal gene flow between the compared populations for a given simulation. For inter-population statistics, the models did have differential explanatory power for the population structure prior to the MWP. Extremely small population sizes most strongly supported panmixia ($1.0 > P > 0.5$) whereas extremely large population sizes favoured complete isolation, demonstrating the sensitivity of the models to both structure and population size. However, for intermediate population sizes, the simulations did not discriminate between each of the three simple models (Fig. 4A). Models incorporating population structure were essential to explain the observed modern population genetic variation, allowing us to rule out panmixia as a possible explanatory model of population history (Fig. 4A). Following the MWP, panmixia was not strongly supported by any modern or fossil comparisons. Instead, strong support was found for some isolation between populations; further, all simulations of population structure provided a best fit under low population sizes (2000). In summary, the observed

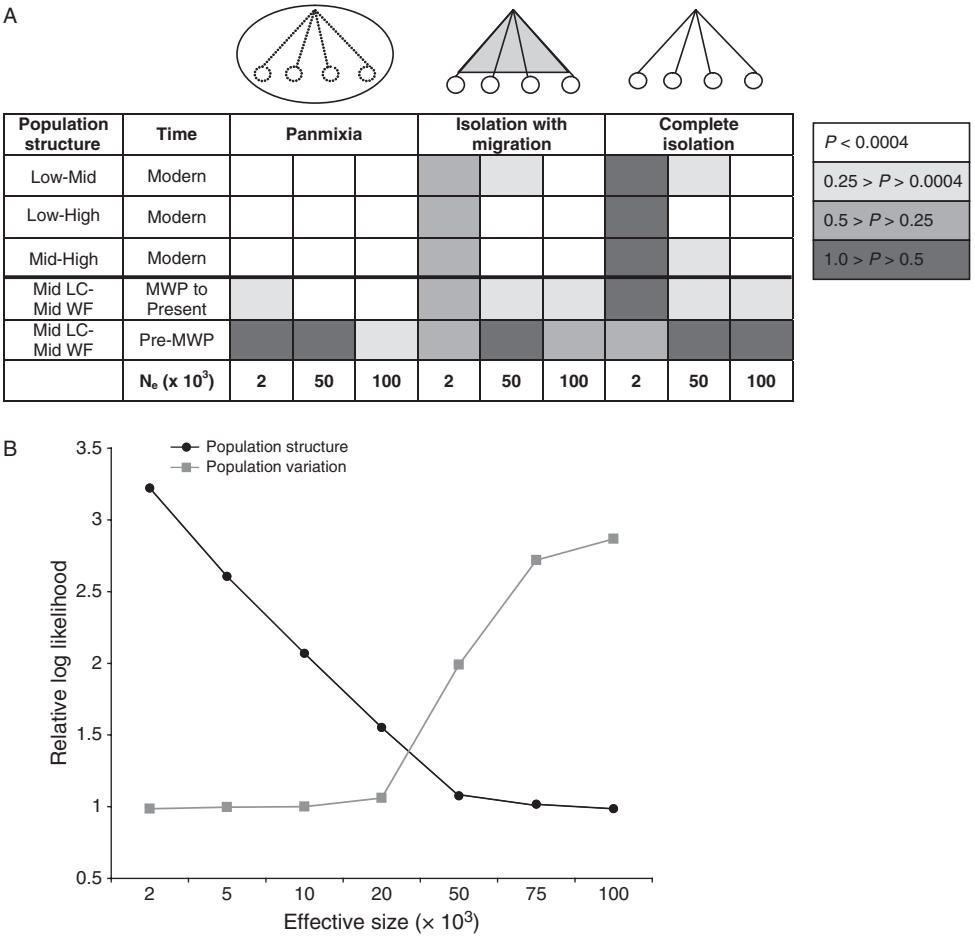

Fig. 4 (A) The probabilities for all the inter-population statistics (F_{ST} values) through space and time. Probabilities are represented using grey shading for all three models of population structure where the highest probability is represented by the darkest shade of grey. (B) Change in relative log-likelihood for population structure (across all 5 inter-population statistics: see text) and population variation (across all 14 intra-population statistics: see text) as a function of effective population size. As the absolute likelihoods (for population structure and genetic variation) are very different (one is based on 5 statistics while the other is based on 14 statistics), we plot the relative likelihood (likelihood divided by the lowest possible value across the effective size range) for both population structure and genetic variation to make inter- and intra-population genetic variation comparable.

genetic differentiation between modern and ancient populations suggested a scenario where population structure may have changed (less structure prior to the MWP) and a situation where, subsequent to the MWP, populations were small and remained generally more isolated since that event.

Relative likelihood values (normalized by the minimal value, complete isolation model) shown in Fig. 4B suggest that models with high effective size (≥50 000) best fit the intra-population statistics, in contrast to the simulation results regarding inter-population statistics that suggest low effective size. This difference between intra and inter-population statistics could be explained by a change in population structure (recent increase in structure and reduction of effective population sizes) subsequent to the MWP. Alternatively, a more complex demographic model that includes asymmetric population sizes (some populations are bigger than others) and asymmetric gene flow (uneven gene flow between populations) could also produce these discrepancies between the intra and interpopulations statistics.

Our results from more complex models (Table 2) revealed that: (i) models with asymmetric population size and gene flow (AIC = 27.3, 38.63) or those that include the impacts of climate (AIC = 38.76, 41.64) fit the data significantly better than the simplistic complete isolation (AIC = 62.4) or isolation with migration (AIC = 67.4) models; (ii) models that include a change in population structure (more structure post-MWP) did not provide a better statistical fit for the data; and (iii) overall, the AIC value was the lowest for models where the central populations were bigger than the peripheral populations, and when gene flow between the central populations was high.

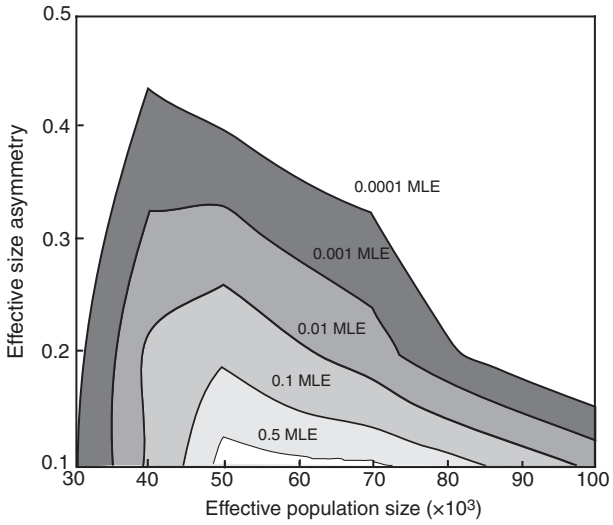

Fig. 5 A contour plot reveals likelihood as a function of effective population size (for the central populations) and size asymmetry (between the central and extreme populations) for the most likely model with four parameters (see Table 2). The minimum log-likelihood or the maximum likelihood estimate (MLE) is observed for a scenario where the size asymmetry is 1:10 and the effective size is 50 000. The plot also shows regions of the parameter space with likelihood values up to 0.5MLE, 0.1MLE, 0.01MLE, 0.001MLE and 0.0001MLE to visualize the uncertainty of this estimation method.

Figure 5 shows the likelihood surface as a function of effective size (of the central populations) and population symmetry (corresponding to the ratio on the effective sizes of the peripheral populations and the central populations). This likelihood surface revealed that effective size is moderately high (between 40 000 and 70 000), but more importantly, the asymmetry between populations is very high, and the likelihood is actually highest when the smallest population is 1/10th the size of the largest populations. There was no support for extremely large (>100 000), extremely small (<10 000) or very similar-sized populations (<1:5).

Discussion

Inferences from phylogenetic and population genetic analyses

Despite relatively recent recolonization of YNP, we found highly significant population structure between populations. Genetic diversity differed significantly between populations with high diversity in the mid-elevation sites and relatively low diversity at the elevational extremes. Furthermore, the ancient and modern genetic data for *Spermophilus armatus* within the GYE revealed that the Yellowstone Plateau was colonized by individuals from all of the major lineages present in the current species distribution – the NWL, NEL and SL. These lineages were not distributed evenly in space or time, leading in part to the observed population structure and variable diversity. For example, although the SL was detected in one modern (Mid site) and two fossil sites, it is not currently found in the populations at the elevational extremes. Therefore, either it was once found throughout the Yellowstone Plateau and is now very restricted, or it never expanded out of the middle elevations around Lamar Valley after colonization. In addition, individuals from the NWL, a lineage now extinct from the current species range, were detected in both ancient sites but not in any of the modern sites. Prior to the MWP, it was in a relatively high frequency at both Lamar Cave and Waterfall Locality (13% and 33% respectively), but appears to have gone extinct on the Yellowstone Plateau as recently as 1000 years BP during or following the climate transition of the MWP. Taken together, the results from the phylyogenetic and population genetic approaches suggest that *S. armatus* experienced two types of genetic change in response to the climatic transition of the MWP: (i) loss of genetic diversity (demonstrated by the extinction of the WF population and the loss of one whole lineage (NWL) from the area and the species range overall); and (iii) change in population structure (as indicated by the AMOVA).

Inferences from simulations

Simulations allowed us to move beyond correlation with climate to compare the likelihoods of alternative population histories given the observed data within a rigorous statistical framework. Our results revealed that the data best fit a model in which the interior, middle elevation populations were a minimum of 10 times larger and experienced much higher gene flow between them than did the populations existing at the elevational extremes of the species range in this region. The degree of population structure might be explained by a source–sink model in which colonies from more optimal habitats maintain larger sizes and higher genetic diversity via high gene flow between them, whereas colonies in marginal environments are small, more isolated and thus more vulnerable to the loss of genetic diversity through drift and other stochastic events leading to local extinction. Furthermore, modelling a change in population structure following the MWP (as suggested by F_{ST}) did not improve our likelihood score. This does not negate any influence of climatic change on these populations, but rather shows that another model (source–sink model) is sufficient to explain the apparent change in genetic structure. However, the loss of

genetic diversity is not easily explained by source–sink dynamics because we would expect recolonization and/or high gene flow between the large, middle elevation populations to sustain genetic diversity through to the present. Together, both our population genetic data and the simulations demonstrate that although the MWP is likely to have reduced genetic diversity, the climatic events of the MWP need not be invoked as the cause of reduction in gene flow between populations or as the catalyst of population structure of the Uinta ground squirrel.

As mentioned above, the simulations indicate high estimates of effective population size (Fig. 5). We caution that these estimates not be interpreted as the local, current effective population size at the Mid site. The presence of three highly divergent lineages in the ancient genetic data of these populations indicates a large ancestral effective size of the individuals that colonized this elevation following deglaciation. Alternatively, as the colonization of these areas began 12 000 years ago, it is possible that there were multiple waves of colonizers from the South preceding our time of sampling. As our ancient genetic data go back 3000 years BP, we cannot (yet) distinguish between these possibilities. It is also possible that the two populations from the Mid site captured a fraction of the genetic population in this region that corresponds to a larger (and unsampled) population. Regardless, genetic variability and thus our estimates of effective size were high in the Mid site prior to the MWP. We also point out that because effective size is high, the time to coalescence precedes the colonization of the GYE. In other words, population processes prior to the colonization of GYE do impact the genetic data we observe. Our modelling approach was specifically aimed at understanding the impacts of population processes over the last 3000 years. We did so by pooling our genetic samples into three windows of time, and by assessing which models best fit the data for each of the three time windows, and for all time windows combined. It is possible that we lacked statistical support for models that include population response to climatic change because such processes are very recent in the context of the whole genealogy. Increasing genetic sampling in the region might refine detection of the impacts of climate.

The source–sink population model revealed by our simulations is also supported by microclimate and ecological data for these same modern populations. For example, the Low and High sites have shorter active seasons and more extreme climates than the Mid site (K. O'Keefe & E. A. Hadly, unpublished). Estimates of extant population size based on capture–recapture data show that the Mid site has 2–3 times more individuals per colony than the Low and High sites (K. O'Keefe & E. A. Hadly, unpublished). The Low and High sites are separated by 1 km or more from other colonies in the vicinity, whereas the Mid site has nearly contiguous colonies throughout the valley (K. O'Keefe & E. A. Hadly, unpublished). Taken together the ecological data suggest that the central Lamar Valley represents more optimal habitat for *S. armatus*, and the more isolated Low and High elevation sites may be serving as sinks (Pulliam 1988). Furthermore, ground surveys for colonies detected several extinct colonies near the Low site (K. O'Keefe, personal observation) and almost complete isolation of the High site from other populations, suggesting that populations at the limits of the species elevational range tend to experience cycles of extirpation and recolonization consistent with sinks. However, it is difficult to distinguish between sources, sinks and pseudo-sink populations (Watkinson & Sutherland 1995) and, in most cases, long-term studies of population parameters (Dias 1996) and studies of emigration and immigration rates (Pulliam & Danielson 1991) are required. Our modelling of the genetic data, albeit informed by our ecological observations, has determined independently that a source–sink system best explains the dynamics of this species in this ecosystem. Furthermore, the modelling identified which populations serve as sources and which are likely to act as sinks.

Our results implicate source–sink population dynamics exacerbated by extrinsic variable environmental conditions across the elevational range of the species in this region. Our phylochronologic data suggest that the Mid site source populations have maintained genetic diversity in the face of climatic change. If source–sink dynamics are typical of the species as a whole, then *S. armatus* may be adapted to withstand perturbations in climate (at least of the magnitude of the MWP). Alternately, changes in climate may drive asymmetry in population size and gene flow between populations, thereby generating source–sink dynamics. Our sampling gradient captures a narrow cross-section from the northern portion of the species range so we do not know if source–sink dynamics predominate throughout the geographic range. Understanding how climatic change may influence a species with metapopulation dynamics requires us to understand the dynamics of populations throughout the range and the spatial features of the landscape (Opdam & Wascher 2004). Because many species are predicted to respond to a changing climate via changes in distribution, the response of metapopulations will likely be more complex than a simple shift in distribution to track cooler climes (Mehlman 1997; Opdam & Wascher 2004). Furthermore, other studies hint that intrinsic life history traits of this species may govern uneven population size

and dispersal in some populations. Previous long-term ecological studies of *S. armatus* elsewhere showed density-dependent dispersal of juveniles (Slade & Balph 1974), suggesting that migration would be asymmetric when density varies. Differentiating between intrinsic vs. extrinsic mechanisms in source–sink dynamics has serious implications for understanding response to climate change in different species, because it suggests that not only species respond uniquely, but also populations of the same species from different parts of the range might respond differently as well.

Finally, we cannot rule out the potential role of selection in producing the pattern of extreme structure in these populations today and following the climate transition the MWP. A McDonald–Kreitman test for neutral molecular evolution was significant (Neutrality Index NI = 6.545, Fisher's exact test, $P = 0.042$; G value = 5.141, $P = 0.023$) and suggestive of negative selection (McDonald & Kreitman 1991), which removes deleterious variation from populations and potentially results in differentiation between populations in different environments (e.g. Storz *et al.* 2007). A pattern suggestive of selection has been found in other intraspecific studies using neutral mitochondrial markers (Bazin *et al.* 2006). Additionally, as we have used mitochondrial data, we acknowledge that our analyses reflect the female lineage. Sex-biased dispersal is known for *Spermophilus* (Slade & Balph 1974; Sauer & Slade 1987). Thus, the complete picture of population history is likely more complex and further analyses using nuclear genetic markers may reveal a different pattern of demography (Waits *et al.* 2000; Hofreiter *et al.* 2001). Increasing genetic data for modern samples (in the form of microsatellite or SNP variation) and inclusion of demographic data (although difficult to obtain) might result in a better-resolved picture for modern populations. Ancient genetic data from more or older sites might also help in better parameterization of the demographic history. Such data would be especially informative for the High and Low sites, from which we lack ancient genetic data. Finally, it is also possible that even more complex models might fit the data better. For example, we could explore models that reveal how multiple, independent colonizations of the Yellowstone ecosystem would have influenced the genetic diversity of the study populations through time. We did not explore these additional data or more complex models as our objective in this paper was to ascertain whether the observed data are representative of population responses to changes in climate (as seen in Hadly *et al.* 2004) or due to complex population demographic processes (such as source–sink dynamics).

In conclusion, our combined analysis of genetic diversity from past and present samples adds temporal information that is typically lacking from population genetic studies. Population genetic analyses of this species revealed that both a loss of genetic diversity and a change in population structure coincided with climatic events of the MWP. Although the MWP is likely to have reduced genetic diversity, our model-testing approach revealed that source–sink dynamics between populations provided a better explanation of the observed data than did a MWP-driven change in gene flow. Thus, our analyses, combined with independent evidence about population demography and environment, provided us details about the ecology of this species that would be undetectable using more traditional methods. Simulation analyses compliment traditional population genetic analyses and in many instances provide a more robust means of analysis because they (i) use the serial coalescent which incorporates geneology; (ii) allow for evolutionary stochasticity; (iii) move beyond correlations to statistically compare alternative models; and (iv) can provide insight into what those alternative models may be. Furthermore, population models such as the source–sink dynamics revealed here are not unique to this species. Thus, our simulation results highlight the important role that underlying demographic processes have on genetic diversity. Such insights into the mechanisms driving patterns of genetic diversity are critical for elucidating species responses to climatic change of the past, present and future.

Acknowledgements

Excellent field help was provided by CN Hill, JE Bruzgul, K Brizgys, M Milne, DM Chow, C von der Ohe, DA Beck, YL Chan and PA Spaeth. Assistance with laboratory work was provided by D Chow and E Martinez. Madhankumar contributed greatly to the processing of the simulation output data. Krishnapriya Tamma replicated the aDNA results in an off-site laboratory. We thank J Blois for help with the maximum likelihood analysis and the D Petrov lab (Stanford University) for use of their lab space to accommodate modern genetic analyses for this project. We gratefully acknowledge the support of J Varley, C Hendrix and the staff of the Yellowstone National Park's Center for Resources. For financial support, we thank the National Center for Environmental Research (NCER) STAR Program, EPA (U915979012 to K O'Keefe), the US National Science Foundation (DEB 0108541 to EA Hadly), the Center for Evolutionary Studies of Stanford University and the Field Studies Program of the Department of Biological Studies, Stanford University. The research conducted for this study complies with the current laws in the USA.

References

Anderson CNK, Ramakrishnan U, Chan YL, Hadly EA (2005) Serial SimCoal: a population genetics model for data from

multiple populations and points in time. *Bioinformatics*, **21**, 1733–1734.

Avise JC (2000) *Phylogeography: The History and Formation of Species*. Harvard University Press, Cambridge, MA.

Barnes I, Matheus P, Shapiro B, Jensen D, Cooper A (2002) Dynamics of Pleistocene population extinctions in Beringian brown bears. *Science*, **5563**, 2267–2269.

Bazin E, Glemin S, Galtier N (2006) Population size does not influence mitochondrial genetic diversity in animals. *Science*, **312**, 570–572.

Belle E, Ramakrishnan UMountainJL, Barbujani G (2006) Serial coalescent simulations suggest a weak genealogical relationship between Etruscans and modern Tuscans. *Proceedings of National Academy of Sciences, USA*, **103**, 8012–8017.

Bruzgul JE, Hadly EA (2006) Non-random patterns in the Yellowstone ecosystem: inferences from mammalian body size, order and biogeographical affinity. *Global Ecology and Biogeography*, **16**, 139–148.

Burnham KP, Anderson DR (2002) *Model Selection and Multimodel Inference: A Practical Information–Theoretic Approach*, 2nd edn. Springer-Verlag, New York.

Chan YL, Anderson CNK, Hadly EA (2006) Bayesian estimation of the timing and severity of a population bottleneck from ancient DNA. *Public Library of Science, Genetics*, **2**, e59; doi: 10.1371/journal.pgne.0020059.

Clement M, Posada D, Crandall K (2000) TCS: a computer program to estimate gene genealogies. *Molecular Ecology*, **9**, 1657–1660.

Dalen L, Nystrom V, Valdiosera C *et al*. (2007) Ancient DNA reveals lack of postglacial habitat tracking in the arctic fox. *Proceedings of the National Academy of Sciences, USA*, **104**, 6726–6729.

Demboski J, Sullivan J (2003) Extensive mtDNA variation within the yellow-pine chipmunk, *Tamias amoenus* (Rodentia: Sciuridae), and phylogeographic inferences for northwest North America. *Molecular Phylogenetics and Evolution*, **26**, 389–408.

Dias PC (1996) Sources and sinks in population biology. *Trends in Ecology and Evolution*, **2**, 326–329.

Drummond AJ, Nicholls GK, Rodrigo AG, Solomon W (2002) Estimating mutation parameters, population history and genealogy simultaneously from temporally spaced sequence data. *Genetics*, **161**, 1307–1320.

Eddingsaas AA, Jacobsen BK, Lessa EP, Cook JA (2004) Evolutionary history of the arctic ground squirrel (*Spermophilus parryi*) in Nearctic Beringia. *Journal of Mammalogy*, **85**, 601–610.

Excoffier L, Laval G, Schneider S (2005) ARLEQUIN, version 3.0: an integrated software package for population genetics data analysis. *Evolutionary Bioinformatics Online*, **1**, 47–50.

Excoffier L, Smouse PE, Quattro JM (1992) Analysis of molecular variance inferred from metric distances among DNA haplotypes: application to human mitochondrial DNA restriction data. *Genetics*, **131**, 479–491.

Fu X (1997) Statistical neutrality of mutations against polyphyly: frequency, causes, and consequences, with insights from animal mitochondrial DNA. *Annual Review of Ecology and Systematics*, **34**, 397–423.

Goosens B, Chikhi L, Ancrenaz M, Lackman-Ancrenaz I, Andau P, Bruford MW (2006) Genetic signature of anthropogenic population collapse in Orang-utans. *PLoS Biology*, **4**, e25; doi: 10.1371/journal.pbio.00400.

Hadly EA (1996) Influence of late-Holocene climate on northern rocky Mountain Mammals. *Quaternary Research*, **46**, 298–310.

Hadly EA (1999) Fidelity of terrestrial vertebrate fossils to a modern ecosystem. *Palaeogeography, Palaeoclimatology, Palaeoecology*, **149**, 389–409.

Hadly EA, van Tuinen M, Chan Y, Heiman K (2003) Ancient DNA evidence of prolonged population persistece with negligible genetic diversity in an endemic Tuco-Tuco. *Journal of Mammalogy*, **84**, 403–417.

Hadly EA, Ramakrishnan U, Chan YL *et al*. (2004) Genetic response to climatic change: insights from ancient DNA and phylochronology. *PLoS Biology*, **2**, 302–319.

Helgen KM, Cole FR, Helgen LE, Wilson DE (2009) Generic revision in the Holarctic ground squirrel Genus *Spermophilus*. *Journal of Mammalogy*, **90**, 270–305.

Hewitt GW (2004) Genetic consequences of climatic oscillations in the Quaternary. *Philosophical Transactions of the Royal Society of London B: Biological Sciences*, **359**, 183–195.

Ho SYW, Phillips MJ, Cooper A, Drummond AJ (2005) Time dependency of molecular rate estimates and systematic overestimation of recent divergence times. *Molecular Evolution Biology*, **22**, 1561–1568.

Hofreiter M, Serre D, Poinar HN, Kuch M, Pääbo S (2001) *Ancient DNA Nature Reviews Genetics*, **2**, 353–359.

Howell AH (1938) *Revision of North American ground squirrels, with a classification of the North American Sciuridae*, North American Fauna No. 56, p. 256. U.S. Department of Agriculture, Washington, DC.

Huelsenbeck JP, Crandall KA (1997) Phylogeny estimation and hypothesis testing using maximum likelihood. *Annual Review in Ecology and Systematics*, **28**, 437–466.

Leonard JA, Wayne RK, Cooper A (2000) Population genetics of Ice Age brown bears. *Proceedings of the National Academy of Sciences, USA*, **97**, 1651–1654.

Leonard JA, Vilà C, Fox-Dobbs K *et al*. (2007) Megafaunal extinctions and the disappearance of a specialized wolf ecomorph. *Current Biology*, **17**, 1146–1150.

McDonald JH, Kreitman M (1991) Adaptive protein evolution at the A*dh* locus in *Drosophila*. *Nature*, **350**, 652–654.

Mehlman D (1997) Change in avian abundance across the geographic range in response to environmental change. *Ecological Applications*, **7**, 614–624.

Millar JS, Zaummuto RM (1983) Life histories of mammals: an analysis of life tables. *Ecology*, **63**, 631–635.

Opdam P, Wascher D (2004) Climate change meets habitat fragmentation: linking landscape and biogeographical scale levels in research and conservation. *Biological Conservation*, **117**, 285–297.

Pierce KL (1979) History and dynamics of glaciation in the northern Yellowstone National Park area. *U.S. Geological Survey Professional Paper*, **729**(F), 91.

Porder SA, Paytan AB, Hadly EA (2003) Mapping the origin of faunal assemblages using strontium isotopes. *Paleobiology*, **29**, 197–204.

Posada D, Crandall KA (1998) MODELTEST: testing the model of DNA substitution. *Bioinformatics*, **14**, 817–818.

Posada D, Crandall K (2001) Intraspecific gene genealogies: trees grafting into networks. *Trends in Ecology & Evolution*, **16**, 37–45.

Pulliam RH (1988) Sources, sinks and population regulation. *The American Naturalist*, **132**, 652–661.

Pulliam RH, Danielson BJ (1991) Sources, sinks and habitat selection: a landscape perspective on population dynamics. *The American Naturalist*, **137**, S50–S66.

Ramakrishnan U, Hadly EA, (2009) Using phylochronology to reveal cryptic population histories: review and synthesis of 29 ancient DNA studies. *Molecular Ecology*, **18**, 1310–1330.

Ramakrishnan U, Hadly EA, Mountain JL (2005) Detecting past population bottlenecks using temporal genetic data. *Molecular Ecology*, **14**, 2915–2922.

Raymond M, Rousset F (1995) An exact test for population differentiation. *Evolution*, **49**, 1280–1283.

Sauer JR, Slade NA (1987) Unita ground squirrels demography: is body mass a better categorical variable than age? *Ecology*, **68**, 642–650.

Simmons MP, Ochoterena H (2000) Gaps as characters in sequence-based phylogenetic analyses. *Systematic Biology*, **49**, 369–381.

Slade NA, Balph DF (1974) Population ecology of Uinta ground squirrels. *Ecology*, **55**, 989–1003.

Soon W, Baliunas S (2003) Proxy climatic and environmental changes of the past 1000 years. *Climate Research*, **23**, 89–110.

Storz JF, Sabatino SJ, Hoffmann FG *et al.* (2007) The molecular basis of high-altitude adaptation in deer mice. *PLoS Genetics*, **3**, e45, 0448–045

Streubel D (1989) *Small Mammals of the Yellowstone Ecosystem*. Robert Rinehart Inc., Boulder.

Swofford DL (2003) PAUP*: *Phylogenetic Analysis Using Parsimony (*and Other Methods)*. Sinauer Associates, Sunderland, MA.

Tajima F (1989a) Statistical method for testing the neutral mutation hypothesis by DNA polymorphism. *Genetics*, **123**, 585–595.

Tajima F (1989b) The effect of change in population size on DNA polymorphism. *Genetics*, **123**, 597–601.

Tamura K, Nei M, Kumar S (2004) Prospects for inferring very large phylogenies by using the neighbor-joining method. *Proceedings of the National Academy of Sciences, USA*, **101**, 11030–11035.

van Tuinen M, O'Keefe K, Ramakrishnan U, Hadly EA (2008) Fire and ice: genetic structure of the Uinta Ground Squirrel (*Spermophilus armatus*) across the Yellowstone Hotspot. *Molecular Ecology*, **17**, 1776–1788.

Valdiosera CE, Nuria G, Anderung C *et al.* (2007) Staying out in the cold: glacial refugia and mitochondrial DNA phylogeography in ancient European brown bears. *Molecular Ecology*, **16**, 5140–5148.

Valdiosera CE, Garcia-Garitagoitia JL, Garcia N *et al.* (2008) Surprising migration and population size dynamics in ancient Iberian brown bears (*Ursus arctos*). *Proceedings of National Academy of Sciences, USA*, **105**, 5123–5128.

Vargas P, Morton CM, Jury SL (1999) Biogeographic patterns in Mediterranean and Macaronesian species of *Saxifraga* (Saxifragaceae) inferred from phylogenetic analyses of ITS sequences. *American Journal of Botany*, **86**, 724–734.

Waits L, Taberlet P, Swenson JE *et al.* (2000) Nuclear DNA microsatellite analysis of genetic diversity and gene flow in the Scandinavian brown bear (*Ursus arctos*). *Molecular Ecology*, **9**, 421–431.

Watkinson AR, Sutherland WJ (1995) Sources, sinks and pseudo-sinks. *The Journal of Animal Ecology*, **64**, 126–130.

Woolley SM, Posada D, Keith A, Crandall KA (2008) A comparison of phylogenetic network methods using computer simulation. *PLoS ONE*, **3**, e1913; doi: 10.1371/journal.pone.0001913.

Zwickl DJ (2006) *Genetic algorithm approaches for the phylogenetic analysis of large biological sequence datasets under the maximum likelihood criterion*. PhD dissertation, The University of Texas at Austin.

Kim O'Keefe is interested in how the ecological and evolutionary characteristics of a species affect its response to climate at different spatial and temporal scales. She is currenly investigating how climate influences population dynamics and genetic structure of ground squirrels. Marcel van Tuinen is assistant professor and curator of the animal frozen tissue bank at UNC Wilmington. His research program focuses broadly on birds and mammals and encompasses the use of ancient DNA for historical population genetic inquiries, fossils for molecular clock calibration, and phylogenomic tools to investigate the tempo and mode of aquatic bird evolution. Uma Ramakrishnan is interested in how genetic variation is partitioned through space and time, and how such variation allows us to understand past demographic processes. She is currently investigating genetic variation and its partitioning for mammals in the Indian subcontinent. Elizabeth A. Hadly studies the ecology and evolution of vertebrates using both fossil and modern assemblages from North America, South America and most recently, India. Her investigations focus on the response of animals to climatic change using genetic, morphological, community, and geochemical analyses.

Supporting information

Additional supporting information may be found in the online version of this article.

Table S1 Sample localities, approximate age, climate interval and the GenBank accession numbers for each haplotype

Table S2 Genetic diversity indices from mtDNA sequences for *Spermophilus armatus* populations

Table S3 Analysis of molecular variance (AMOVA) among test groupings of potential populations of *Spermophilus armatus* in Yellowstone National Park

Please note: Wiley-Blackwell are not responsible for the content or functionality of any supporting information supplied by the authors. Any queries (other than missing material) should be directed to the corresponding author for the article.